Research Article | Vol. 27, No. 3 | 4 Feb 2019 | OPTICS EXPRESS 1825
Optics EXPRESS

Timing the release of the correlated electrons in strong-field nonsequential double ionization by circularly polarized two-color laser fields

XIAOMENG MA,[1] YUEMING ZHOU,[1,*] YINBO CHEN,[1] MIN LI,[1] YANG LI,[1] QINGBIN ZHANG,[1,3] AND PEIXIANG LU[1,2]

[1] *Wuhan National Laboratory for Optoelectronics and School of Physics, Huazhong University of Science and Technology, Wuhan 430074, China*
[2] *Hubei Key Laboratory of Optical Information and Pattern Recognition, Wuhan Institute of Technology, Wuhan 430205, China*
[3] *zhangqingbin@hust.edu.cn*
[*] *zhouymhust@hust.edu.cn*

Abstract: With the semiclassical ensemble model, we systematically investigate the correlated electron dynamics in strong-field nonsequential double ionization (NSDI) by the counter-rotating circularly polarized two-color (CPTC) laser pulses. Our results show that the angular distributions of the electrons in NSDI sensitively depend on the intensity ratio of the CPTC laser fields. At the small ratio, the electron pairs emit with a relative angle of about 120°, and this angle shifts to 40° as the ratio increases and finally it exhibits a wide range distribution as the intensity ratio further increases. Back analysis of the NSDI trajectories shows that this behavior results from the relative-intensity-dependence of the release time of the electron pairs in the CPTC laser fields. The release times of the electron pairs are directly mapped to the angular distribution. Our results indicate that the emission times of the correlated electrons in NSDI can be controlled with the CPTC laser fields.

1. Introduction

Atoms or molecules exposed to an intense laser field might be tunnel ionized. The tunneling ionized electron may be driven back to the parent ion by the oscillating electric field of the laser pulses [1] and trigger various interesting phenomena, such as high-order above-threshold ionization [2, 3], high-order harmonic generation (HHG) [4, 5], photoelectron holography [6–8] and nonsequential double ionization (NSDI) [9, 10]. Revealing the details of the underlying dynamics and exploring their applications is one of the main missions of the contemporary attosecond science. Particularly, in NSDI the electron pairs exhibit highly correlated behavior and during the past decades extensive efforts have been performed on NSDI to reveal the microscopic dynamics of the correlated electrons [11–20]. Generally, there are two pathways in NSDI, i.e., recollision-impact ionization (RII) where the bound electron is ionized immediately after recollision, and recollision excitation with subsequent ionization (RESI) where the bound electron is excited by recollision and ionized by the subsequent electric field after recollision [21]. Recent experimental and theoretical studies have provided deep insights into the details of electron dynamics, for instance, the role of ion-electron interaction and final state electron-electron repulsion [22, 23], the asymmetric energy sharing during recollision [24], the wavelength-dependent electron dynamics [25, 26], the pulse-duration effect [27, 28] and the atom/molecule species dependence of the electron correlation in NSDI [29, 30].

Another very important issue in strong-field double ionization is the emission times of the electrons. Accurate determination of the emission time of the electron in strong-field ionization is of fundamental importance in the attosecond science. Plenty of efforts have been performed in this

#346479 https://doi.org/10.1364/OE.27.001825
Journal © 2019 Received 21 Sep 2018; revised 19 Dec 2018; accepted 21 Dec 2018; published 22 Jan 2019

Optics EXPRESS

topic. For example, for the RII pathway of NSDI, it was usually accepted that the two electrons leave the core immediately after recollision. While our recent theoretical study has shown that even in the RII pathway, there is considerable part of NSDI events where the bound electrons are ionized with time delay of several hundred attoseconds after recollision [31]. This delayed emission in the RII pathway was confirmed by a recent experiment [32]. In RESI at low laser intensities, it has been demonstrated that double ionization occurs through recollision-induced doubly excited state [33], wherein a relative time of about 200 attoseconds between the emissions of the two electrons was revealed by analyzing the correlated electron momentum spectrum. Knowledge about the emission time is crucial for fully understanding the electron correlation in NSDI.

In strong-field ionization, various methods have been proposed to time the release of electron from atoms and molecules. In particular, the attoclock is a very effective technique to record the release time of electron in strong-field tunneling ionization [34, 35]. Based on the angular streaking, in the attoclock experiment an elliptically polarized laser field is employed to ionize the atom/molecule. The release time is directly mapped to the angular distribution of the photoelectron. Thus, by analyzing the angular distribution of the photoelectron, the release time of the electron in strong-field tunneling ionization can be determined with the accuracy as high as a few attoseconds. This technique has been extended to study the ionization times of the two electrons in strong-field double ionization. With this attoclock technique, the sequential nature of double ionization in the elliptical laser field and the release times of the two electrons have been unambiguously determined [36–38]. For some peculiar species, recollision can still happen even in the circularly polarized (CP) laser fields [39–41]. In this case, this attoclock technique has been successful in tracing the release times of the electron pair in NSDI [41]. More generally, recollision is forbidden in the laser field with the large ellipticity and thus NSDI is strongly suppressed. Thus, the attoclock technique is difficult to record the release times of the correlated electron pairs in NSDI.

Recently, it has been proposed and demonstrated that the counter-rotating circularly polarized two-color (CPTC) laser fields can drive recollision in strong-field ionization [42–45]. This laser field has been used to drive HHG in producing circularly polarized EUV [46–48] and soft-x-ray beam [49]. In NSDI, the electron dynamics driven by the counter-rotating CPTC laser fields have also been studied, both theoretically and experimentally [50–53]. Similar to the elliptically/circularly polarized laser field in the attoclock experiment, this CPTC laser field also possesses the property of angular streaking and thus it can be used to trace the release times of the two electrons after recollision in NSDI. Thus, in this paper, with the semiclassical ensemble model, we systematically study the correlated electron dynamics in NSDI driven by the counter-rotating CPTC laser fields and we focus on the angular distributions of the correlated electrons. Our results show that the relative emission angle of the electron pairs depends on the intensity ratio of the CPTC laser fields. Back analysis of the NSDI trajectories shows that it results from the intensity-ratio dependence of time delay between the emissions of the two electrons after recollision. Thus, our study indicates that the CPTC can be used to time the release of the correlated electrons in recollision induced NSDI.

2. The semiclassical ensemble model

Due to the huge computational requirements of numerically solving the time-dependent Schrödinger equation for multi-electron systems in strong laser fields [19, 54], in the past decades numerous theoretical studies on NSDI have resorted to the classical and semiclassical methods. It has been demonstrated that the classical and semiclassical models are very successful not only in explaining the experimental results [24, 55, 56] but also in predicting various phenomena in strong-field double ionization [57]. Moreover, classical and semiclassical ensemble models enable one to trace the trajectory from the beginning to the end of the laser pulse, and

Optics EXPRESS

thus provide an intuitive picture on the ionization processes of the two electrons [20, 24, 57]. Therefore, here we employ the two-dimensional semiclassical ensemble model to study the electron dynamics of the NSDI by the counter-rotating CPTC laser fields [55, 56].

In this model, the outer electron is ionized through tunneling [58]. It has zero initial parallel velocity (parallel to the transient electric field of the laser pulse) and a Gaussian transverse velocity distribution [59]. The weight of each trajectory is evaluated by $w(t_0, \upsilon^i_{\perp 0}) = w(t_0)w(\upsilon^i_{\perp 0})$, in which

$$w(t_0) = \left(\frac{2(2I_{p1})^{1/2}}{|\mathbf{E}(t_0)|}\right)^{\frac{2}{\sqrt{2I_{p1}}}-1} \exp\left(\frac{-2(2I_{p1})^{3/2}}{3|\mathbf{E}(t_0)|}\right), \tag{1}$$

$$w(\upsilon_{\perp 0}) = \frac{1}{|\mathbf{E}(t_0)|}\exp\left(-\frac{(\upsilon_{\perp 0})^2(2I_{p1})^{1/2}}{|\mathbf{E}(t_0)|}\right). \tag{2}$$

Here t_0 is the tunneling time, $\upsilon_{\perp 0}$ the initial transverse momentum and $\mathbf{E}(t_0)$ is the transient electric field of the laser pulse at tunneling. For the bound electron, the initial position and momentum are depicted by the microcanonical distribution. After tunneling ionization of the outer electron, the subsequent evolution of the two electrons in the combined Coulomb and laser fields is described by the classical Newtonian equation (atomic units are used throughout until stated otherwise):

$$\frac{\mathrm{d}^2\mathbf{r}_\mathrm{i}}{\mathrm{d}t^2} = -\nabla[V_{ne}(\mathbf{r}_i) + V_{ee}(\mathbf{r}_1, \mathbf{r}_2)] - \mathbf{E}(t), \tag{3}$$

where the index i denotes the label of the two electrons, and $\mathbf{r}_i$ refers to the electron coordinates. $V_{ne}(\mathbf{r}_i) = -2/\sqrt{\mathbf{r}_i^2 + a^2}$ and $V_{ee}(\mathbf{r}_1, \mathbf{r}_2) = 1/\sqrt{(\mathbf{r}_1 - \mathbf{r}_2)^2 + b^2}$ are the nucleus-electron and electron-electron interaction potentials, respectively. In our calculations, the first and second ionization potentials are chosen as $I_{p1} = 0.28$ a.u. and $I_{p2} = 0.55$ a.u., respectively, to match those of Mg. The soft parameter a is employed to avoid autoionization when both electrons are in the proximity of the nucleus and also to speed up our calculations [60–62]. In our calculations, we set $a = 3.0$ and $b = 0.05$. Here the value of b is not important as long as it is small enough (it can be set to be zero).

The electric field of the CPTC pulse is written as $\mathbf{E}(t) = \mathbf{E}_1(t) + \mathbf{E}_2(t)$, where

$$\mathbf{E}_1(t) = \frac{\gamma_E E_0}{\sqrt{2}(1+\gamma_E)} f(t)[\cos(\omega_1 t)\hat{\mathbf{x}} + \sin(\omega_1 t)\hat{\mathbf{y}}], \tag{4}$$

and

$$\mathbf{E}_2(t) = \frac{E_0}{\sqrt{2}(1+\gamma_E)} f(t)[\cos(\omega_2 t)\hat{\mathbf{x}} - \sin(\omega_2 t)\hat{\mathbf{y}}]. \tag{5}$$

Here, ω_1 and ω_2 are the angular frequencies of the two fields, respectively. γ_E is electric field amplitude ratio between the two laser pulses (the intensity ratio can be written as $\gamma_I = {\gamma_E}^2$ accordingly). In our calculations, we vary the ratio γ_E of the two fields while keep the sum of the intensities of these two fields (0.05 PW/cm^2) unchanged [i.e., E_0 in Eqs. (4) and (5) is unchanged] [43, 50–52]. The laser fields are polarized in the x-y plane. $f(t)$ is the pulse envelope which is taken as

$$f(t) = \begin{cases} 1, & t \le 8\mathrm{T}_1 \\ \cos^2\left(\dfrac{(t-8\mathrm{T}_1)\pi}{4\mathrm{T}_1}\right), & 8\mathrm{T}_1 < \mathrm{t} \le 10\mathrm{T}_1 \\ 0, & t > 10\mathrm{T}_1 \end{cases} \tag{6}$$

where T_1 is the optical period of the fundamental laser field $\mathbf{E}_1(t)$.

Optics EXPRESS

In our calculations, several millions weighted classical two-electron trajectories are traced from the tunneling moment to the end of the pulse, resulting in more than 10^4 double ionization (DI) events for each relative ratio γ_E. We define the event as double ionization when the energies of both electrons are positive at the end of the laser pulses.

We mention that in our calculations we will not consider focal averaging of the laser pulses. In a previous theoretical paper on HHG the focal volume effect has been considered and it has been shown that this effect could smooth the oscillations in the helicity of the harmonic spectrum [48]. In this paper, we focused on the angular distributions of the electron from NSDI and study the correspondence between the release time and the angular of the electrons' final momentum. This correspondence does not depend on the intensities of the laser pulses and thus the laser focal volume effect should be less significant. The agreement between our numerical results and previous experimental data shown below further supports the validity of our work.

3. Results and discussions

Figure 1 shows the double ionization yields as a function of the ratio γ_E at different wavelengths. It is shown that the double ionization of Mg in the CPTC laser fields occurs over a broad range of γ_E. The double ionization yield strongly depends on γ_E and exhibits a pronounced peak at certain values of γ_E, depending on the wavelengths of the driving fields. For example, in the 400-nm + 800-nm, 800-nm + 1600-nm, and 1000-nm + 2000-nm CPTC laser fields (the ratio of the wavelengths of the two fields $\lambda_2/\lambda_1 = 2.0$), the double ionization yield reaches a maximum at around $\gamma_E = 2.0$. For the ratio $\lambda_2/\lambda_1 = 1.5$ (800-nm + 1200-nm) and $\lambda_2/\lambda_1 = 2.5$ (800-nm + 2000-nm), the yields peak at $\gamma_E = 1.5$ and 2.5 respectively. Closer inspection shows that for the cases of $\lambda_2/\lambda_1 = 2.0$, the location of the peak changes a little with the wavelengths. For instance, in the 400-nm + 800-nm field, it locates at $\gamma_E = 1.7$. This is in consistent with previous experiments on NSDI of Ar by the CPTC fields where it is shown that the double ionization yield

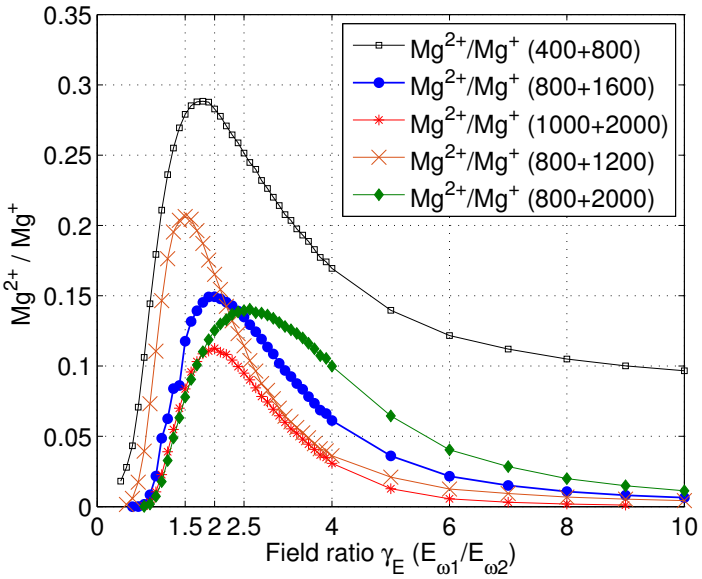

Fig. 1. The yields of double to single ionization versus γ_E ($\gamma_E = E_{\omega_1}/E_{\omega_2}$) at a combined intensity of $I_0 = 0.05$ PW/cm^2. The wavelengths of the two-color components are labeled in the legend.

Optics EXPRESS

peaks at 1.5 or 1.7 [43,51]. As the wavelength increases, the peak is more close to $\gamma_E = 2.0$. This behavior could be understood qualitatively as following. According to the simple-man model [1], in the CPTC fields recollision could occur for the tunneled electron with zero initial velocity when γ_E equals to the wavelength ratio λ_2/λ_1. While for other values of γ_E, it requires a proper nonzero initial velocity for the tunneled electron to return back. Consequently, the recollision is most probable and thus the NSDI yield maximizes when γ_E equals to the wavelength ratio λ_2/λ_1. When the Coulomb interaction between the tunneled electron and the parent ion is taken into account, the value of γ_E for the most probable recollision should shift from the value predicted by the simple-man model. For short wavelengths, the Coulomb interaction plays an important role in the recollision process and thus this shift is more obvious, as shown by the data for the 400-nm + 800-nm fields. As the wavelength increases, the Coulomb interaction becomes less important. Consequently, the NSDI yield peaks at γ_E more close to the value predicted by the simple-man model.

To obtain more details about the correlated electron dynamics, we analyze the angular distribution of the photoelectrons. We take the cases of 800-nm + 1600-nm fields with $\gamma_E = 1.0$, 2.0, and 3.5 as examples and analyze the angular distributions of the correlated electron pairs. The left column of Fig. 2 displays the angular momentum distributions of the electrons from the NSDI events (red dots). Note that the two electrons cannot be distinguished in experiments and thus here both electrons are included when we perform statistical analysis of the angular distributions. These distributions are experimentally accessible. For comparison, we also display the angular distribution of the electrons from the singly ionized (SI) events, as shown by the black circles. In the SI events, the electrons release around the maxima of the electric field of the laser pulses, and the electron angular distributions of the SI events can serve as the time mark. For $\gamma_E = 1.0$, there is a small angular shift between the distributions for the NSDI and SI events, as shown in Fig. 2(a). At larger γ_E, the angular shift becomes more obvious, as shown in Figs. 2(b) and 2(c). These indicate that in the NSDI events the release time of the electrons is different from that in the SI events.

In a recent experiment, the electron momentum distributions for the single ionization and NSDI by the CPTC laser fields have been analyzed, where the shift between the angular distribution of the electron from single ionization events and that of the recolliding electron in NSDI events has been reported [43]. It is in agreement with our numerical result at $\gamma_E = 1.0$. It means that the angular shift is visible even with the focal averaging on the laser intensity. In that experimental paper, the microscopic electron dynamics in NSDI by the CPTC field have been inferred. In this paper, with the semiclassical ensemble model we reveal the electron dynamics intuitively, as shown below.

In our theoretical model, we can distinguish the two electrons. In the right column of Fig. 2, we separately show the angular distributions of the recolliding and the bound electrons of the NSDI events, from which more details of the ionization dynamics could be inferred. At $\gamma_E = 1.0$, the angular distributions of the recolliding and the bound electrons are very different. For the recolliding electron (the blue curve), the peaks of the distribution shift a little from those of the SI events (the black dots), and the widths of these peaks are much narrower than those of the SI case. While for the bound electron (the green curve), the positions and the widths of the peaks are much closer to those of the SI events. These behaviors reveal rich information about the ionization dynamics of NSDI in the CPTC fields, as explained below. The recolliding electron is ionized through tunneling and it can be expected that its angular distribution should be similar to that of the SI electrons if there is no recollision. In NSDI, however, all of the tunneled electrons experience recollision. The shift in the angular distributions of the recolliding electron and SI events results from the recollision. This shift is small. It means that the trajectories of the recolliding electrons are not disturbed too much. It indicates that the recollision is soft recollision, i.e., the recolliding electron only transfers a small part of its energy to the parent ion when it

Optics EXPRESS

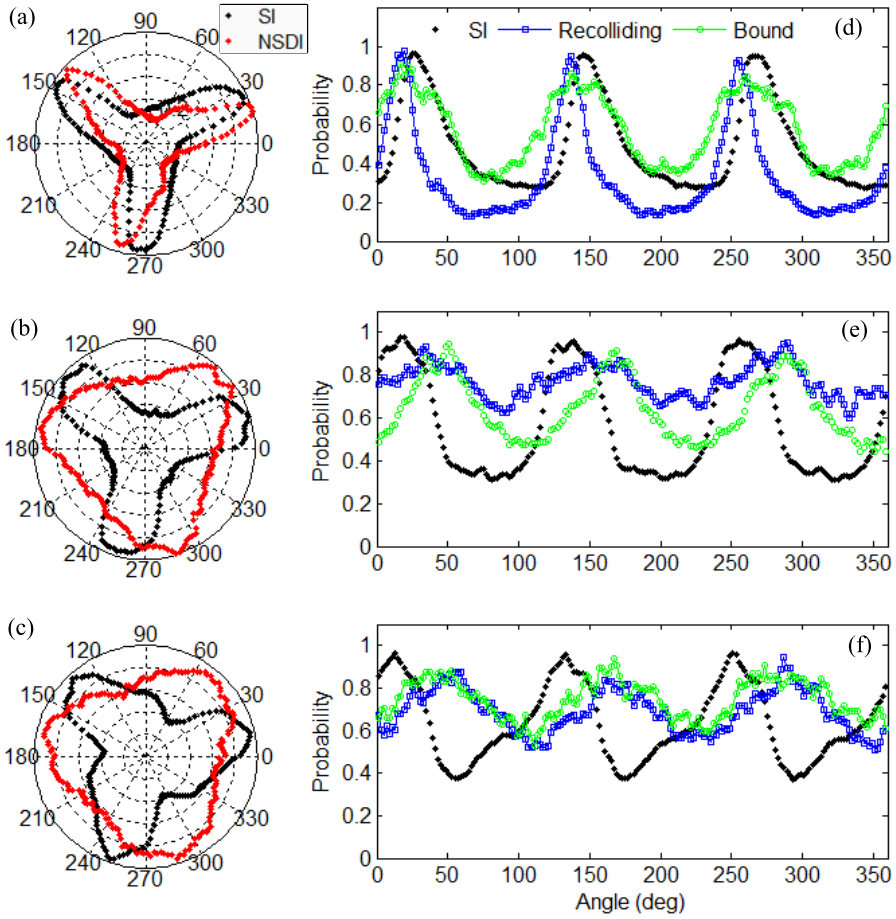

Fig. 2. (a)-(c) The emitting angle distributions of the electrons for the SI (black dots) and NSDI events (red dots) for the cases of γ_E = (a) 1.0, (b) 2.0, and (c) 3.5 for the counter-rotating CPTC fields consisting of the 800-nm and 1600-nm pulses, respectively. (d)-(f) The emitting angle distribution of the electrons for the SI and NSDI events. Here we separately show the distribution for the recolliding and the bound electrons. The black dots represent the electrons in the SI event.

passes by. This is easy to understand. According to the simple-man model, recollision most probably occurs at $\gamma_E = 2.0$. At $\gamma_E = 1.0$, the recollision condition is not exactly satisfied and thus there is a relatively large impact parameter for the recollision. Consequently, the recolliding electron is only slightly disturbed by the recollision, leading to the small angular shift between the recolliding and the SI electrons. The narrowing of angular distribution for the recolliding electron is due to the fact that only a selective part of the tunneled electrons could return to the parent ion and lead to NSDI. Because of the soft recollision, only a small amount of energy is transfered to the bound electron. Thus, the bound electron is ionized through the RESI pathway, i.e., it is ionized by the laser field near the peak of the electric field after recollision. Therefore, the angular distribution of the bound electron is similar to that of the SI events.

The above analysis of the electron angular distribution provides us an informative picture of

Optics EXPRESS

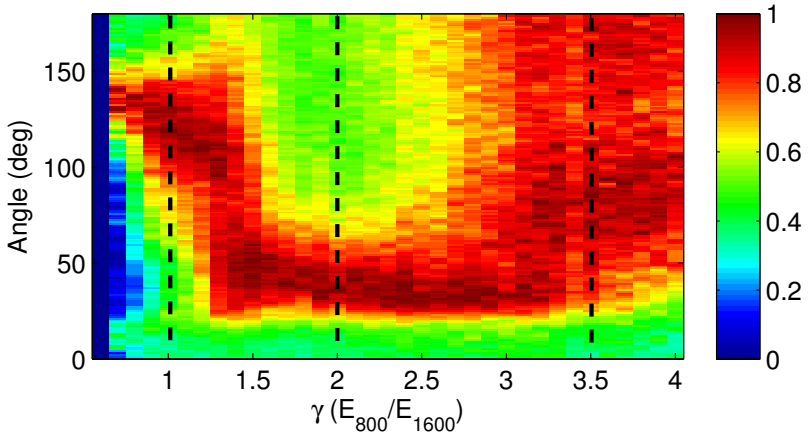

Fig. 3. Distribution of relative emitting angle between the two electrons as a function of the amplitude ratio γ_E for the CPTC fields consisting of the 800-nm and 1600-nm pulses. The black dashed lines indicate the cases of $\gamma_E = 1.0, 2.0$, and 3.5, respectively, which are analyzed in Figs. 4 and 5.

the NSDI dynamics. It indicates that at $\gamma_E = 1.0$ the soft recollision is prevalent. The bound electron is excited by this soft recollision and subsequently ionized by the electric field through a tunneling-like process. The trajectories of the recolliding electrons are only slightly affected by the recollision. The different angular distributions of the recolliding and the bound electron mean that the memories about the electrons' dynamics before recollision survive in the recollision process.

As γ_E increases, the angular distributions of the recolliding and bound electrons become more similar, as shown in Fig. 2(e) where $\gamma_E = 2.0$. It indicates that the recollision is more effective. In this case, the first tunneled electron can be more easily driven back to the parent ion by the laser field. Consequently, the hard recollision becomes prevalent, wherein the energy transferred and exchanged between the two electrons is more efficient. The hard recollision clears the memories of the electrons and thus the two electron become more indistinguishable in the angular distributions. At $\gamma_E = 3.5$, the returning energy of the recolliding electron is very small [43] and thus the energy transfer in the recollision process is more effective. Therefore, the recollision clears all of the memories of the electrons, leading to the same angular distributions of the two electrons, as shown in Fig. 2(f). Figures 2(e) and 2(f) show that the angular distributions of the electrons peak at different angles for the NSDI and SI events. It indicates the different release times of electrons in the SI and NSDI events.

Experimentally, the two electrons in NSDI are indistinguishable. Despite of this, insightful information about the correlated electron dynamics can be inferred from the relative emitting angular distribution of the electron pairs, which is accessible in experiments. Figure 3 shows the relative emitting angular distribution of the two electrons in NSDI as a function of the ratio γ_E. It is shown that the distribution sensitively depends on γ_E. At $\gamma_E = 0.8$, the relative angle between the two electrons is centered at about 125°. As γ_E increases, the distribution gradually moves to smaller value and it peaks at 43° as γ_E increases to 1.7. When γ_E further increases, the distribution moves towards larger value and broadens. These distributions indicate the γ_E-dependence of the relative emission time of the two electrons, as will be shown below.

For ionization by circularly polarized laser fields, there is a simple relation between the relative angle $\Delta\theta$ and the time delay Δt of the sequential release of the two electrons, $\Delta\theta = \omega\Delta t$ (ω is the

Optics EXPRESS

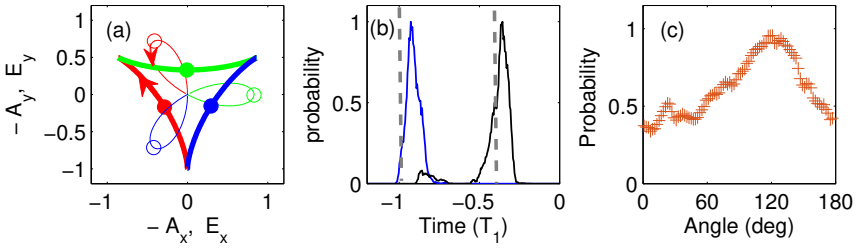

Fig. 4. (a) The electric field $\mathbf{E}(t)$ (thin curves) and the corresponding negative vector potential -$\mathbf{A}(t)$ (thick curves) of the TCCP field with $\gamma_E = 1.0$ (plotted in arbitrary units). The arrows indicate the time evolution direction. A lobe of the electric field corresponds to a side of the triangle of the negative vector potential. The dots mark the field maxima and their corresponding negative vector potentials. (b) The blue curve is the final ionization time of the first electron after recollision and the black curve is the final ionization time of the second electron. T_1 indicates the optical cycle of 800-nm laser field. The vertical gray dashed lines represent the field maxima. Here we only selected the events where tunneling ionization of the recolliding electron occurs within one lobe of the electric field and recollision occurs at its first returning. (c) The relative angle distribution of the electron pairs.

frequency of the circular laser pulse) [38]. For our TCCP fields, this relation is not so intuitive. In order to explore the correspondence between the relative angular distribution and the release times of the electron pairs, we again take $\gamma_E = 1.0$, 2.0 and 3.5 as examples and trace the NSDI trajectories. We find out the recollision time and final ionization time of the two electrons after recollision. Here, the recollision time is defined as the instant of the closest approach of the two electrons after the tunneling ionization of the recolliding electron and the final ionization time is defined as the instant when the electron achieves positive energy after recollision.

We first analyze the case of $\gamma_E = 1.0$. Figure 4(a) shows the electric field (the thin curve) and vector potential (the thick curve) of the laser field. The electric field exhibits a trefoil-like shape. The electron tunneling ionizes around one lobe of the trefoil and then returns to the parent ion near the next lobe [53]. Figure 4(b) shows the final ionization time of the recolliding and the bound electron after ionization. Here we only consider the NSDI events where the recollisiosn of the electrons occur at their first returning. Note that the final ionization time of the recolliding electron is coincident as the recollision time because at $\gamma_E = 1.0$ the soft recollision dominates wherein the energy of the recolliding electron is always positive during the recollision process, i.e., the blue curve in Fig. 4(b) also represents the recollision time distribution. It is shown that the bound electron is ionized around the following peak of the electric field after recollision. It means RESI is the dominant process. The peak around 120° in relative emitting angular distribution shown in Fig. 4(c) directly reveals this process. It indicates that the two electron are released around the successive lobes of the electric field in tunneling-like processes. It also indicates that the recollision hardly influences the emitting angle of the recolliding electron. Thus, by analyzing the observable relative emitting angle of the electron pairs, the underlying dynamics can be inferred.

We now turn to the cases of $\gamma_E = 2.0$ and 3.5. The electric field (the thin curves) and vector potential (the thick curves) of the laser pulses for $\gamma_E = 2.0$ and 3.5 are shown in Figs. 5(a) and 5(b), respectively. The electric fields also exhibit the three-lobe structure but the lobes become wider as γ_E increases. Figure 5(c) shows the relative emitting angle distributions of the electron pairs and Fig. 5(d) displays the distributions of the time delay between the final ionization of the two electrons after recollision. It is shown that the relative angle distributions for these two

Optics EXPRESS

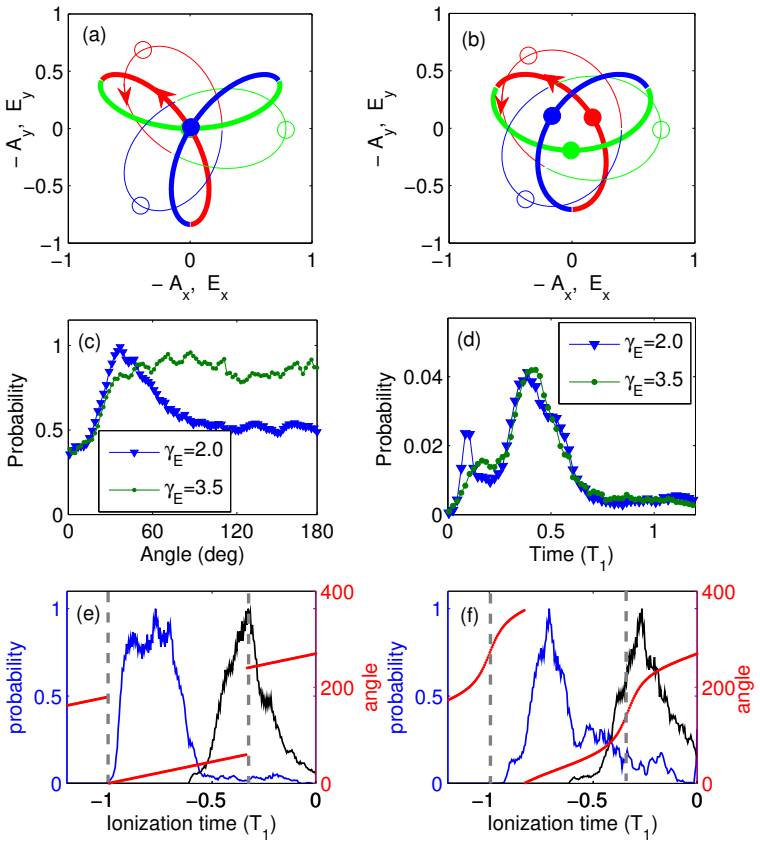

Fig. 5. (a) (b) The electric field $\mathbf{E}(t)$ (thin curves) and the corresponding negative vector potential $-\mathbf{A}(t)$ (thick curves) of the CPTC pulse with $\gamma_E = 2.0$ and 3.5, respectively (plotted in arbitrary units). The arrows indicate the time evolution direction. The dots mark the field maxima and their corresponding negative vector potentials. (c) The relative emitting angle distribution of the electron pairs. (d) The distributions of the time delay between the final ionization of the two electrons after recollision. (e) (f) Left axis: the distribution of the final ionization of the two electrons after recollision. Right axis (the red curve): The direction of the vector potential $-\mathbf{A}(t)$. The gray dashed lines indicate the field maximum. The blue curves and the black curves indicate the ionization times of the first and the second electron, respectively.

cases are very different though the time delay distributions are very similar. For $\gamma_E = 2.0$ the relative angle distribution exhibits a pronounce peak at 40° while at $\gamma_E = 3.5$ it exhibits the almost uniformly distribution between 40° and 180°. This seems counterintuitive.

To understand this behavior, we show the final ionization time distributions of the two electrons after recollision in Figs. 5(e) and 5(f). The direction of the vector potential of the CPTC field as a function of time is also shown here (the right axis). The direction of the vector potential indicates the angle of the final momentum if the electron ionizes with negligible velocity. For $\gamma_E = 2.0$, the two electrons ionize around $t_i = -0.65T_1$ and $-0.25\mathrm{T}_1$ (T_1 indicates the optical cycle of 800-nm laser field), respectively. The relative angle between the directions of the vector potential at these instants is about 40°, which is in consistent with the relative angle of the electron pairs.

Optics EXPRESS

It indicates that indeed the relative angle is related to the time delay between the final ionization of the two electrons. For $\gamma_E = 3.5$, though the ionization times of the two electrons are almost the same as those at $\gamma_E = 2.0$, the directions of the vector potential of the CPTC field at these instants in Fig. 5(f) are very different from those in Fig. 5(e). The vector potential direction changes sharply around the ionization instant of the second electron. Thus, the electron release near this instant has a very wide distribution in the final momentum angle. This explains the almost uniform distribution between $40° \sim 180°$ of the relative emitting angle of the electron pairs shown in Fig. 5(c).

The analysis above shows that the relative angular momentum distribution indeed could provide rich information about the ionization dynamics of NSDI, especially the relative release time of the electron pairs after recollision. Though the relation between the relative angle and the release time of the electron is not as simple as those in the circularly polarized laser field, the information could be obtained by comparing the angular distribution with the vector potential of the laser fields.

4. Conclusions

In conclusion, we have theoretically studied the correlated electron dynamics in NSDI driven by the counter-rotating CPTC laser fields. We show that the electron angular distribution could provide much information about the dynamics of NSDI in the CPTC laser fields. By analyzing the relative emitting angle of the electron pairs, the information about the time delay between the release of the two electrons after recollision could be obtained. The correspondence of the relative emitting angle and the time delay of the two electrons release in the CPTC fields depend on the relative strength of the two fields, which can be easily established by analyzing the vector potential of the CPTC pulses. Though this correspondence is more intricate than that in the circularly polarized laser field, it can be used to study the release time of NSDI in the target where recollision is forbidden in the circular laser field. Thus, one can study, for example, the species dependence of the release time of the excited or doubly excited states induced by recollision. We hope our study will inspire further experimental studies on this issue.

Funding

National Natural Science Foundation of China (NSFC) (11874163, 11622431, 61475055, 11604108, 11627809); Program for HUST Academic Frontier Youth Team.

Acknowledgments

Numerical simulations presented in this paper were carried out using the High Performance Computing Center experimental testbed in SCTS/CGCL (see http://grid.hust.edu.cn/hpcc).

References

1. P. B. Corkum, "Plasma perspective on strong field multiphoton ionization," Phys. Rev. Lett. **71**(13), 1994-1997(1993).
2. W. Becker, F. Grasbon, R. Kopold, D. Milošević, G. Paulus, and H. Walther, "Above-threshold ionization: From classical features to quantum effects," Adv. At. Mol. Opt. Phys. **48**(1979), 35-98 (2002).
3. J. Tan, Yang Li, Y. Zhou, M. He, Y. Chen, M. Li, and P. Lu, "Identifying the contributions of multiple-returning recollision orbits in strong-field above-threshold ionization," Opt. Quant. Electron. **50**(2), 57 (2018).
4. A. McPherson, G. Gibson, H. Jara, U. Johann, T. S. Luk, I. A. McIntyre, K. Boyer, and C. K. Rhodes, "Studies of multiphoton production of vacuum-ultraviolet radiation in the rare gases," J. Opt. Soc. Am. B **4**(4), 595-601 (1987).
5. M. Ferray, A. L′Huillier, X. F. Li, L. A. Lompré, G. Mainfray and C. Manus, "Multiple-harmonic conversion of 1064 nm radiation in rare gases," J. Phys. B **21**(3), L31 (1988).
6. Y. Zhou, O. I. Tolstikhin, and T. Morishita, "Near-forward rescattering photoelectron holography in strong-field ionization: extraction of the phase of the scattering amplitude," Phys. Rev. Lett. **116**(17), 173001 (2016).
7. M. He, Y. Li, Y. Zhou, M. Li, W. Cao, and P. Lu, "Direct visualization of valence electron motion using strong-field photoelectron holography," Phys. Rev. Lett. **120**(13), 133204 (2018).

Optics EXPRESS

8. J. Tan, Y. Zhou, M. He, Y. Chen, Q. Ke, J. Liang, X. Zhu, M. Li, and P. Lu, "Determination of the ionization time using attosecond photoelectron interferometry," Phys. Rev. Lett. **121**(25), 253203 (2018).
9. D. N. Fittinghoff, P. R. Bolton, B. Chang, and K. C. Kulander, "Observation of nonsequential double ionization of helium with optical tunneling," Phys. Rev. Lett. **69**(18), 2642-2645 (1992).
10. B. Walker, B. Sheehy, L. F. DiMauro, P. Agostini, K. J. Schafer, and K. C. Kulander, "Precision measurement of strong field double ionization of helium," Phys. Rev. Lett. **73**(9), 1227-1230 (1994).
11. Th. Weber, H. Giessen, M. Weckenbrock, G. Urbasch, A. Staudte, L. Spielberger, O. Jagutzki, V. Mergel, M. Vollmer, and R. Dörner, "Correlated electron emission in multiphoton double ionization," Nature (London) **405**(6787), 658-661 (2000).
12. R. Moshammer, B. Feuerstein, W. Schmitt, A. Dorn, C. D. Schröter, and J. Ullrich, "Momentum Distributions of Ne^{n+} Ions Created by an Intense Ultrashort Laser Pulse," Phys. Rev. Lett. **84**(3), 447-450 (2000).
13. M. Weckenbrock, D. Zeidler, A. Staudte, Th. Weber, M. Schöffler, M. Meckel, S. Kammer, M. Smolarski, O. Jagutzki, V. R. Bhardwaj, D. M. Rayner, D. M. Villeneuve, P. B. Corkum, and R. Dörner, "Fully Differential Rates for Femtosecond Multiphoton Double Ionization of Neon," Phys. Rev. Lett. **92**(21), 213002 (2004).
14. A. Rudenko, K. Zrost, B. Feuerstein, V. L. B. de Jesus, C. D. Schröter, R. Moshammer, and J. Ullrich, "Correlated Multielectron Dynamics in Ultrafast Laser Pulse Interactions with Atoms," Phys. Rev. Lett. **93**(25), 253001 (2004).
15. X. Liu, H. Rottke, E. Eremina, W. Sandner, E. Goulielmakis, K. O. Keeffe, M. Lezius, F. Krausz, F. Lindner, M. G. Schätzel, G. G. Paulus, and H. Walther, "Nonsequential Double Ionization at the Single-Optical-Cycle Limit," Phys. Rev. Lett. **93**(26), 263001 (2004).
16. Y. Liu, L. Fu, D. Ye, J. Liu, M. Li, C. Wu, Q. Gong, R. Moshammer, and J. Ullrich, "Strong-Field Double Ionization through Sequential Release from Double Excitation with Subsequent Coulomb Scattering," Phys. Rev. Lett. **112**(1), 013003 (2014).
17. J. Chen and C. H. Nam, "Ion momentum distributions for He single and double ionization in strong laser fields," Phys. Rev. A **66**(5), 053415 (2002).
18. C. Figueira de Morisson Faria, H. Schomerus, X. Liu, and W. Becker, "Electron-electron dynamics in laser-induced nonsequential double ionization," Phys. Rev. A **69**(4), 043405 (2004).
19. J. S. Parker, B. J. S. Doherty, K. T. Taylor, K. D. Schultz, C. I. Blaga, and L. F. DiMauro, "High-Energy Cutoff in the Spectrum of Strong-Field Nonsequential Double Ionization," Phys. Rev. Lett. **96**(13), 133002 (2006).
20. X. Ma, Y. Zhou, P. Lu, "Multiple recollisions in strong-field nonsequential double ionization," Phys. Rev. A **93**(1), 013425 (2016).
21. B. Feuerstein, R. Moshammer, D. Fischer, A. Dorn, C. D. Schröter, J. Deipenwisch, J. R. Crespo López-Urrutia, C. Höhr, P. Neumayer, J. Ullrich, H. Rottke, C. Trump, M. Wittmann, G. Korn, and W. Sandner, "Separation of Recollision Mechanisms in Nonsequential Strong Field Double Ionization of Ar: The Role of Excitation Tunneling," Phys. Rev. Lett. **87**(4), 043003 (2001).
22. A. Staudte, C. Ruiz, M. Schöffler, S. Schössler, D. Zeidler, Th. Weber, M. Meckel, D. M. Villeneuve, P. B. Corkum, A. Becker, and R. Dörner, "Binary and Recoil Collisions in Strong Field Double Ionization of Helium," Phys. Rev. Lett. **99**(26), 263002 (2007).
23. Y. Zhou, C. Huang, and P. Lu, "Coulomb-tail effect of electron-electron interaction on nonsequential double ionization," Phys. Rev. A **84**(2), 023405 (2011).
24. Y. Zhou, Q. Liao, and P. Lu, "Asymmetric electron energy sharing in strong-field double ionization of helium," Phys. Rev. A **82**(5), 053402 (2010).
25. P. Kaminski, R. Wiehle, W. Kamke, H. Helm, and B. Witzel, "Wavelength dependence of double ionization of xenon in a strong laser field," Phys. Rev. A **73**(1), 013413 (2006).
26. Y. Wang, S. Xu, Y. Chen, H. Kang, X. Lai, W. Quan, X. Liu, X. Hao, W. Li, S. Hu, J. Chen, W. Becker, W. Chu, J. Yao, B. Zeng, Y. Cheng, and Z. Xu, " Wavelength scaling of atomic nonsequential double ionization in intense laser fields," Phys. Rev. A **95**(6), 063415 (2017).
27. M. Kübel, K. J. Betsch, N. G. Kling, A. S. Alnaser, J. Schmidt, U. Kleineberg, Y. Deng, I. Ben-Itzhak, G. G. Paulus, T. Pfeifer, J. Ullrich, R. Moshammer, M. F. Kling, and B. Bergues, "Non-sequential double ionization of Ar: from the single- to the many-cycle regime," New J. Phys. **16**(3), 033008 (2014).
28. Y. Chen, Y. Zhou, Y. Li, M. Li, P. Lan, and P. Lu, "The contribution of the delayed ionization in strong-field nonsequential double ionization," J. Chem. Phys. **144**(2), 024304 (2016).
29. E. Eremina, X. Liu, H. Rottke, W. Sandner, M. G. Schätzel, A. Dreischuh, G. G. Paulus, H. Walther, R. Moshammer, and J. Ullrich, "Influence of Molecular Structure on Double Ionization of N_2 and O_2 by High Intensity Ultrashort Laser Pulses," Phys. Rev. Lett. **92**(17), 173001 (2004).
30. A. Rudenko, K. Zrost, B. Feuerstein, V. L. B. de Jesus, C. D. Schröter, R. Moshammer, and J. Ullrich, "Correlated Multielectron Dynamics in Ultrafast Laser Pulse Interactions with Atoms," Phys. Rev. Lett. **93**(25), 253001 (2004).
31. Q. Li, Y. Zhou, and P. Lu, "Universal time delay in the recollision impact ionization pathway of strong-field nonsequential double ionization," J. Phys. B: At. Mol. Opt. Phys. **50**(22), 225601 (2017).
32. H. Kang, Y. Zhou, and P. Lu, "Steering electron correlation time by elliptically polarized femtosecond laser pulses," Opt. Express **26**(25), 33400-33408 (2018).
33. N. Camus, B. Fischer, M. Kremer, V. Sharma, A. Rudenko, B. Bergues, M. Kübel, N. G. Johnson, M. F. Kling, T. Pfeifer, J. Ullrich, and R. Moshammer, "Attosecond correlated dynamics of two electrons passing through a transition state," Phys. Rev. Lett. **108**(7), 073003 (2012).

Optics EXPRESS

34. P. Eckle, A. N. Pfeiffer, C. Cirelli, A. Staudte, R. Dörner, H. G. Muller, M. Büttiker, U. Keller, "Attosecond Ionization and Tunneling Delay Time Measurements in Helium," Science **322**(5907), 1525-1529 (2008).
35. L. Torlina, F. Morales, J. Kaushal, I. Ivanov, A. Kheifets, A. Zielinski, A. Scrinzi, H. G. Muller, S. Sukiasyan, M. Ivanov, and O. Smirnova, "Interpreting attoclock measurements of tunnelling times," Nat. Phys. **11**(6), 503-508 (2015).
36. A. N. Pfeiffer, C. Cirelli, M. Smolarski, R. Dörner and U. Keller, "Timing the release in sequential double ionization," Nat. Phys. **7**(5), 428-433 (2011).
37. Y. Zhou, C. Huang, Q. Liao, and P. Lu, "Classical Simulations Including Electron Correlations for Sequential Double Ionization," Phys. Rev. Lett. **109**(5), 053004 (2012).
38. X. Wang, J. Tian, and J. H. Eberly, "Angular Correlation in Strong-Field Double Ionization under Circular Polarization," Phys. Rev. Lett. **110**(7), 073001 (2013).
39. G. D. Gillen, M. A. Walker, and L. D. Van Woerkom, "Enhanced double ionization with circularly polarized light," Phys. Rev. A **64**(4), 043413 (2001).
40. F. Mauger, C. Chandre, and T. Uzer, "Recollisions and Correlated Double Ionization with Circularly Polarized Light," Phys. Rev. Lett. **105**(8), 083002 (2010).
41. A. H. Winney, S. K. Lee, Y. F. Lin, Q. Liao, P. Adhikari, G. Basnayake, H. B. Schlegel, and W. Li, "Attosecond Electron Correlation Dynamics in Double Ionization of Benzene Probed with Two-Electron Angular Streaking," Phys. Rev. Lett. **119**(12), 123201 (2017).
42. C. A. Mancuso, D. D. Hickstein, K. M. Dorney, J. L. Ellis, E. Hasović, R. Knut, P. Grychtol, C. Gentry, M. Gopalakrishnan, D. Zusin, F. J. Dollar, X. Tong, D. B. Milošević, W. Becker, H. C. Kapteyn, and M. M. Murnane, "Controlling electron-ion rescattering in two-color circularly polarized femtosecond laser fields," Phys. Rev. A **93**(5), 053406 (2016).
43. S. Eckart, M. Richter, M. Kunitski, A. Hartung, J. Rist, K. Henrichs, N. Schlott, H. Kang, T. Bauer, H. Sann, L. Ph. H. Schmidt, M. Schöffler, T. Jahnke, and R. Dörner, "Nonsequential Double Ionization by Counterrotating Circularly Polarized Two-Color Laser Fields," Phys. Rev. Lett. **117**(13), 133202 (2016).
44. K. Lin, X. Jia, Z. Yu, F. He, J. Ma, H. Li, X. Gong, Q. Song, Q. Ji, W. Zhang, H. Li, P. Lu, H. Zeng, J. Chen, and J. Wu, "Comparison Study of Strong-Field Ionization of Molecules and Atoms by Bicircular Two-Color Femtosecond Laser Pulses," Phys. Rev. Lett. **119**(20), 203202 (2017).
45. A. Gazibegović-Busuladžić, W. Becker, and D. B. Milošević, "Helicity asymmetry in strong-field ionization of atoms by a bicircular laser field," Opt. Express **26**(10), 12684-12697 (2018).
46. A. Fleischer, O. Kfir, T. Diskin, P. Sidorenko, and O. Cohen, "Spin angular momentum and tunable polarization in high-harmonic generation," Nat. Photonics **8**(7), 543-549 (2014).
47. O. Kfir, P. Grychtol, E. Turgut, R. Knut, D. Zusin, D. Popmintchev, T. Popmintchev, H. Nembach, J. M. Shaw, A. Fleischer, H. Kapteyn, M. Murnane, and O. Cohen, "Generation of bright phase-matched circularly-polarized extreme ultraviolet high harmonics," Nat. Photonics **9**(2), 99-105 (2015).
48. D. B. Milošević, "Control of the helicity of high-order harmonics generated by bicircular laser fields," Phys. Rev. A **98**(3), 033405 (2018).
49. T. Fan, P. Grychtol, R. Knut, C. Hernández-García, D. D. Hickstein, D. Zusin, C. Gentry, F. J. Dollar, C. A. Mancuso, C. W. Hogle, O. Kfir, D. Legut, K. Carva, J. L. Ellis, K. M. Dorney, C. Chen, O. G. Shpyrko, E. E. Fullerton, O. Cohen, P. M. Oppeneer, D. B. Milošević, A. Becker, A. A. Jaroń-Becker, T. Popmintchev, M. M. Murnane, and H. C. Kapteyn, "Bright circularly polarized soft X-ray high harmonics for X-ray magnetic circular dichroism," Proc. Natl. Acad. Sci. U.S.A. **112**(46), 14206-14211 (2015).
50. J. L. Chaloupka and D. D. Hickstein, "Dynamics of Strong-Field Double Ionization in Two-Color Counterrotating Fields," Phys. Rev. Lett. **116**(14), 143005 (2016).
51. C. A. Mancuso, K. M. Dorney, D. D. Hickstein, J. L. Chaloupka, J. L. Ellis, F. J. Dollar, R. Knut, P. Grychtol, D. Zusin, C. Gentry, M. Gopalakrishnan, H. C. Kapteyn, and M. M. Murnane, "Controlling Nonsequential Double Ionization in Two-Color Circularly Polarized Femtosecond Laser Fields," Phys. Rev. Lett. **117**(13), 133201 (2016).
52. S. Ben, P. Y. Guo, X. F. Pan, T. T. Xu, K. L. Song, and X. S. Liu, "Recollision induced excitation-ionization with counter-rotating two-color circularly polarized laser field," Chem. Phys. Lett. **679**, 38-44 (2017).
53. C. Huang, M. Zhong, and Z. Wu, "Intensity-dependent two-electron emission dynamics in nonsequential double ionization by counter-rotating two-color circularly polarized laser fields," Opt. Express **26**(20), 26045-26056 (2018).
54. S. Hu, "Boosting Photoabsorption by Attosecond Control of Electron Correlation," Phys. Rev. Lett. **111**(12), 123003 (2013).
55. D. Ye, X. Liu, and J. Liu, "Classical Trajectory Diagnosis of a Fingerlike Pattern in the Correlated Electron Momentum Distribution in Strong Field Double Ionization of Helium," Phys. Rev. Lett. **101**(23), 233003 (2008).
56. L. Fu, G. Xin, D. Ye, and J. Liu, "Recollision Dynamics and Phase Diagram for Nonsequential Double Ionization with Circularly Polarized Laser Fields," Phys. Rev. Lett. **108**(10), 103601 (2012).
57. Y. Zhou, C. Huang, A. Tong, Q. Liao, and P. Lu, "Correlated electron dynamics in nonsequential double ionization by orthogonal two-color laser pulses," Opt. Express **19**(3), 2301-2308 (2011).
58. M. V. Ammosov, N. B. Delone, and V. P. Krainov, "Tunnel Ionization Of Complex Atoms And Atomic Ions In Electromagnetic Field," Zh. Eksp. Teor. Fiz. **91**, 2008-2013 (1986).
59. N. B. Delone and V. P. Krainov, "Energy and angular electron spectra for the tunnel ionization of atoms by strong low-frequency radiation," J. Opt. Soc. Am. B **8**(6), 1207-1211 (1991).

Optics EXPRESS

60. N. Li, Y. Zhou, X. Ma, M. Li, C. Huang, and P. Lu, "Correlated electron dynamics in strong-field nonsequential double ionization of Mg," J. Chem. Phys. **147**(17), 174302 (2017).
61. S. Luo, X. Ma, H. Xie, M. Li, Y. Zhou, W. Cao, and P. Lu, "Controlling nonsequential double ionization of Ne with parallel-polarized two-color laser pulses," Opt. Express **26**(10), 13666-13676 (2018).
62. X. Ma, Y. Zhou, N. Li, M. Li, P. Lu, "Attosecond control of correlated electron dynamics in strong-field nonsequential double ionization by parallel two-color pulses," Optics & Laser Technology **108**, 235-240 (2018).